Volume 53
Number 8
28 February 2024
Pages 3419-3894

Dalton Transactions

An international journal of inorganic chemistry

rsc.li/dalton

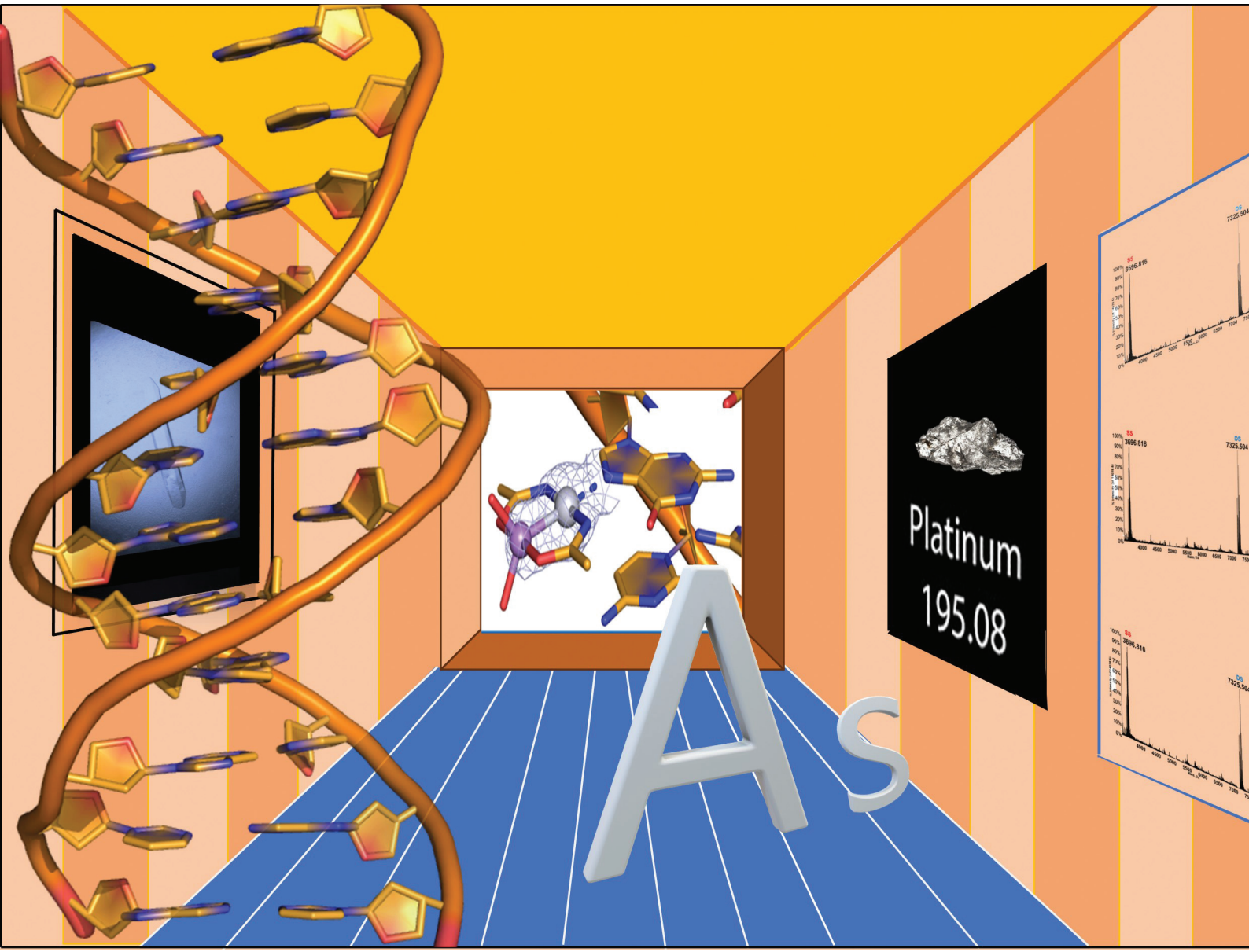

ISSN 1477-9226

ROYAL SOCIETY OF CHEMISTRY

PAPER

Antonello Merlino *et al.*

On the mechanism of action of arsenoplatins: arsenoplatin-1 binding to a B-DNA dodecamer

Dalton Transactions

ROYAL SOCIETY OF CHEMISTRY

PAPER

View Article Online
View Journal | View Issue

Check for updates

Cite this: *Dalton Trans.*, 2024, **53**, 3476

On the mechanism of action of arsenoplatins: arsenoplatin-1 binding to a B-DNA dodecamer†

Romualdo Troisi, ‡[a,b] Gabriella Tito, ‡[a] Giarita Ferraro, [a] Filomena Sica, [a] Lara Massai, [c] Andrea Geri,[c] Damiano Cirri, [d] Luigi Messori [c] and Antonello Merlino *[a]

Received 21st December 2023,
Accepted 11th January 2024

DOI: 10.1039/d3dt04302a

rsc.li/dalton

The reaction of Pt-based anticancer agents with arsenic trioxide affords robust complexes known as arsenoplatins. The prototype of this family of anticancer compounds is arsenoplatin-1 (AP-1) that contains an $As(OH)_2$ fragment linked to a Pt(II) moiety derived from cisplatin. Crystallographic and spectrometric studies of AP-1 binding to a B-DNA double helix dodecamer are presented here, in comparison with cisplatin and transplatin. Results reveal that AP-1, cisplatin and transplatin react differently with the DNA model system. Notably, in the AP-1/DNA systems, the Pt–As bond can break down with time and As-containing fragments can be released. These results have implications for the understanding of the mechanism of action of arsenoplatins.

Introduction

Although the serendipitous discovery of the anticancer properties of cisplatin occurred more than 50 years ago,[1] even today cisplatin and its main derivatives carboplatin and oxaliplatin are among the most important anticancer agents. These drugs are used in the treatment of 40–50% of all cancer patients, as single agents or in combination with other molecules.[2–4] Although these Pt-based drugs are extensively used in the clinics, their administration is associated with a number of undesirable side effects.[5–8] Accordingly, many new Pt[9–13] and non-Pt[14–17] metal-based potential drugs have been synthesized to overcome the limitations of Pt-based therapy. Proteins,[18,19] liposomes,[20,21] supramolecular organometallic complexes,[22] and other alternative drug delivery systems[23–26] were also studied. However, cisplatin, carboplatin, oxaliplatin, and arsenic trioxide[27] remain the only metal-based drugs approved by the U.S. Food and Drug Administration for cancer treatment: these drugs trigger apoptosis in cancer cells. Pt-based drugs act through direct Pt binding to nuclear DNA;[6,28] As_2O_3 targets zinc-fingers and/or other cysteine-rich proteins, causing intense oxidative stress.[29–34] It has been shown that cisplatin and As_2O_3 can have synergistic effects on ovarian cancer cells.[23,35,36] In an effort to design compounds that combine the Pt and As moieties of the above drugs, O'Halloran and coworkers synthesized a new class of compounds called arsenoplatins.[37] These compounds contain a robust Pt–$As(OH)_2$ bond with an expected square planar Pt(II) geometry, but an unusual five coordinate As(III) geometry. Arsenoplatins are cytotoxic for several cancer cell lines and have a distinct mechanism of action when compared to cisplatin and As_2O_3.[37,38]

In vitro evaluation of a single dose of the prototype of the arsenoplatin family (AP-1, $[Pt(\mu\text{-}NHC(CH_3)O)_2ClAs(OH)_2]$, Fig. 1) against the NCI 60 tumor cell panel screen revealed that it is more cytotoxic than either cisplatin or As_2O_3 in about half of the tested cancer cell lines.[39]

It has been shown that AP-1 is able to bind the model proteins hen egg white lysozyme and bovine pancreatic ribonuclease forming adducts where the metal-bound fragment

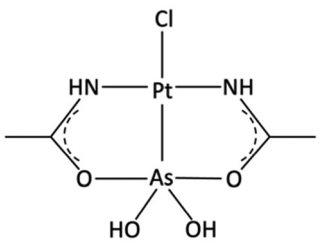

Fig. 1 Structure of the arsenoplatin-1 (AP-1) complex.

[a]*Department of Chemical Sciences, University of Naples Federico II, Complesso Universitario di Monte Sant'Angelo, via Cintia, 80126 Naples, Italy. E-mail: antonello.merlino@unina.it*
[b]*Institute of Biostructures and Bioimaging, CNR, via Pietro Castellino 111, 80131 Naples, Italy*
[c]*Department of Chemistry "U. Schiff", University of Florence, via della Lastruccia 3, 50019 Sesto Fiorentino, Italy*
[d]*Department of Chemistry and Industrial Chemistry (DCCI), University of Pisa, Via Giuseppe Moruzzi 13, 56124 Pisa, Italy*

†Electronic supplementary information (ESI) available: Experimental section: materials; crystallization; data collection, structure determination, refinement, and structural analysis; electrospray ionization mass spectrometry experiments. ESI Tables S1–S3. ESI Fig. S1–S7. See DOI: https://doi.org/10.1039/d3dt04302a

‡These authors contributed equally to this work.

retains the Pt–As core.[39] However, it is also able to bind proteins upon releasing the arsenic center, as observed in the case of the adducts formed upon reaction with myoglobin and glyceraldehyde 3-phosphate dehydrogenase.[40]

AP-1 also binds DNA, as judged by ICP-MS analysis.[39] In AP-1/DNA adducts the Pt/As ratio increases over time due to the gradual release of the $As(OH)_2$ moiety.[39] This behavior makes arsenoplatins potent prodrugs capable of delivering As_2O_3 to solid tumors.

To further validate this assertion and characterize in more detail the interaction between arsenoplatins and DNA, here we report the crystal structure of the adduct formed upon reaction of AP-1 with a B-DNA dodecamer model system,[41,42] *i.e.*, the Dickerson sequence 5′-CGCGAATTCGCG-3′ that has been used to describe the primary mode of binding of cisplatin to a B-DNA.[41] In Dickerson's duplex structure, three Pt binding sites were found, close to the N7 position of guanines 4, 10 and 16.[41] To directly compare the structure of the AP-1/DNA adduct with that formed by the same DNA double helical dodecamer with cisplatin, the cisplatin/DNA structure was here re-solved and re-refined. The AP-1/DNA and cisplatin/DNA structures were also compared with those of the adducts obtained upon reaction of the same DNA sequence with transplatin, which is inactive against cancer cells.[43] Finally, to gain further independent information on the investigated systems, ESI MS measurements were carried out.

Results and discussion

Structure of a new cisplatin/DNA adduct

Crystals of cisplatin/DNA, transplatin/DNA and AP-1/DNA adducts were obtained using the soaking strategy. Crystals of $d(5'\text{-CGCGAATTCGCG-}3')_2$ were grown as previously described[44] and the adducts with cisplatin, transplatin and AP-1 were obtained under the same conditions, *i.e.* exposing the crystals to solutions containing the metal compounds (see the Experimental section). Crystals of the DNA adduct with cisplatin diffract X-rays at a resolution of 2.31 Å. The statistics of the final model are listed in Table S1.† Unexpectedly, the cisplatin/DNA adduct structure, which was refined with an *R*-factor value of 0.231 (and an *R*-free value of 0.266), shows four Pt centers (Fig. 2A and Table S2†) bound to Gua4, Gua10, Gua16, and Gua22 (Fig. 3 and Fig. S1†). Thus, a new Pt binding site (Gua22), not observed by Dickerson and coworkers,[41] was found in the present structure. In all four sites, Pt ligands cannot be confidently modelled, since the cisplatin fragment retains a large conformational freedom upon coordination to the N7 atom. The occupancy factors for the Pt atoms in this structure are 0.60, 0.50, 0.50, and 0.65, for the Pt bound to Gua4, Gua10, Gua16, and Gua22, respectively. The *B*-factors are within the range of 72–85 $Å^2$, while the average Pt–N7 distance is 2.2 Å.

Structures of transplatin/DNA adducts

The literature data showed that cisplatin and transplatin react differently with DNA, with the *cis* isomer inducing larger

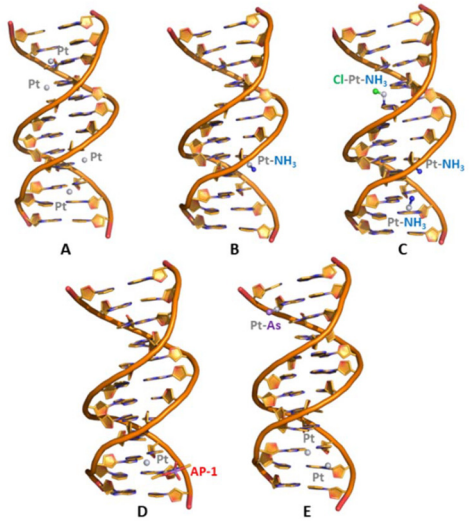

Fig. 2 View of (A) the cisplatin/DNA adduct (PDB code: 8C62), (B) the transplatin/DNA adduct obtained after 48 h of soaking (PDB code: 8RI5), (C) the transplatin/DNA adduct obtained after 7 days of soaking (PDB code: 8RI3) (D), the AP-1/DNA adduct obtained after 4 h of soaking (PDB code: 8C63) and (E) AP-1/DNA adduct obtained after 48 h of soaking (PDB code: 8C64).

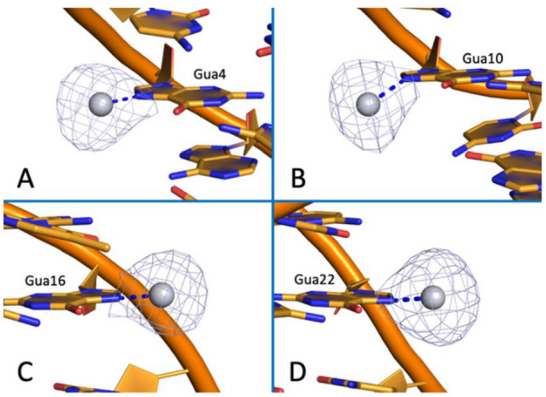

Fig. 3 Pt binding sites in the cisplatin/DNA adduct here reported. Pt centers are found close to (A) Gua4, (B) Gua10, (C) Gua16, and (D) Gua22. $2F_o - F_c$ electron density maps were recorded at 1.0σ. Anomalous difference electron density maps are presented in Fig. S1.†

effects on the DNA structure.[43,45–47] Since AP-1 has a structure that is more similar to transplatin than to cisplatin, structural data on the interaction of transplatin and B-DNA were collected, so that transplatin could be used as a suitable reference for AP-1 reactivity with DNA. Crystallographic data on the transplatin/DNA adducts were obtained over time by solving the crystal structures of the adducts formed after 48 h and 7 days. The overall structures of the double helix in the adducts (Fig. 2B and C) are similar to each other and to that in the adduct with cisplatin. The root-mean-square deviation between the atoms of the three structures is within the range 0.60–0.70 Å. The structures, solved at 1.41 Å and 1.40 Å resolution, refined with *R*-factor values of 0.189 and 0.218 (*R*-free =

0.229 and 0.256), showed the binding of Pt atoms to Gua16 and Gua4 + Gua10 + Gua16 for the crystals exposed to transplatin for 48 h and 7 days, respectively (Fig. 4, Fig. S2, and Table S2†). Both structures have been replicated with very similar results (unpublished data). As in the case of the DNA adduct with cisplatin, Pt ligands cannot be confidently modelled. However, an NH_3 group was tentatively added close to Pt in all the detected binding sites with the exception of Gua4, where a Cl^- ligand could also be present. The occupancy factors for the Pt atoms in these structures are 0.20 for Gua16 in the structure obtained after 48 h of soaking, and 0.25, 0.30, and 0.30 for the Pt bound to Gua4, Gua10, and Gua16 in the structure obtained after 7 days of soaking. The *B*-factors are within the range 27–65 $Å^2$.

These findings indicate that transplatin and cisplatin share the same Pt binding sites, with transplatin forming DNA adducts with lower Pt occupancies.

Structures of AP-1/DNA adducts

Structural data on the interaction of AP-1 and B-DNA were also obtained over time. The structures of AP-1/DNA adducts were solved using crystals exposed to the metallodrug for 4 and 48 h. The structures were refined at 1.52 Å and 2.51 Å resolution with *R*-factor values of 0.238 and 0.179 (*R*-free = 0.261 and 0.232). The structure obtained after 4 h of soaking has been replicated with very similar results (unpublished data). A search in the Protein Data Bank (Table S3†) reveals that our structures represent the first molecular models of adducts formed by DNA with heterobimetallic Pt-based compounds. The overall structures of the double helix in the AP-1/DNA adducts (Fig. 2D and E) are not significantly affected by the metal compound binding. The root-mean-square deviation between the atoms of the two structures and those of DNA with cisplatin and transplatin is within the range 0.60–0.74 Å. However, a deeper comparison between the structures reveals significant differences.

In the AP-1/DNA structure obtained after 4 h (AP-1/DNA 4 h) of soaking (Fig. 2D), only two metal binding sites can be identified (Fig. 5A, B and Fig. S3, Table S2†). Metal centers are found close to N7 atoms of Gua10 (Fig. 5A) and Gua14 (Fig. 5B). In the former site (Gua10), which the structure of AP-1/DNA shares with that of cisplatin/DNA, only a Pt atom was found (Fig. 5A). Interestingly, in the latter metal binding site (Gua14), that was not identified in our structure and in the published structure of cisplatin/DNA,[41] the Pt–As bond was retained (Fig. 5B). Close to Gua14, metal ligands were generously modelled, considering the residual electron density around the metal centers and the compound geometry. However, the assignments should be considered with care. The occupancy factor for the Pt atoms bound to Gua10 and Gua14 in this structure is 0.20. The *B*-factors are 57.9 and 39.3 $Å^2$, respectively. The Pt–N7 bond distances in the two sites are similar (2.2 and 2.0 Å); the Pt–As bond length is 2.2 Å.

In the AP-1/DNA structure obtained after 48 h (AP-1/DNA 48 h) of soaking (Fig. 2E), three metal binding sites were identified (Fig. 5C–E and Fig. S3, Table S2†). The first two sites coincide with those observed in the AP-1/DNA 4 h structure (Gua10 and Gua14) (Fig. 5C and D). Interestingly, only a Pt atom was found close to both these sites. Since after 4 h of soaking both Pt and As were observed close to Gua14, the comparison between the two structures obtained after 4 and 48 h suggests that the Pt–As bond is broken with time upon DNA binding. A third metal binding site was identified close to the N7 atom of Gua2 (Fig. 5E). This site was not identified in our and previous[41] DNA adducts with cisplatin. Here, the Pt–As

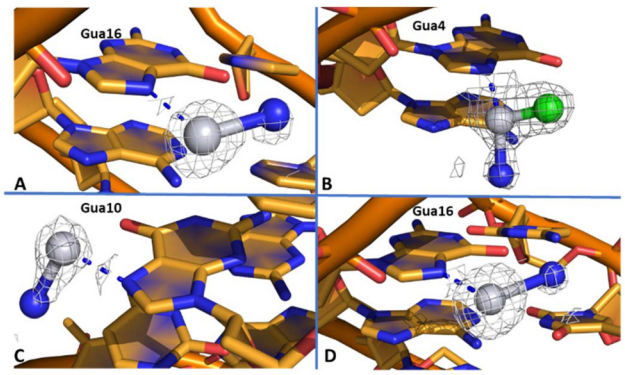

Fig. 4 Pt binding sites in the transplatin/DNA adduct after 48 h and 7 days of soaking. Pt centers are found upon 48 h close to (A) Gua16, and upon 7 days close to (B) Gua4, (C) Gua10, and (D) Gua16. $2F_o - F_c$ electron density maps are reported at 1.0σ in grey. Anomalous difference electron density maps are presented in Fig. S2.†

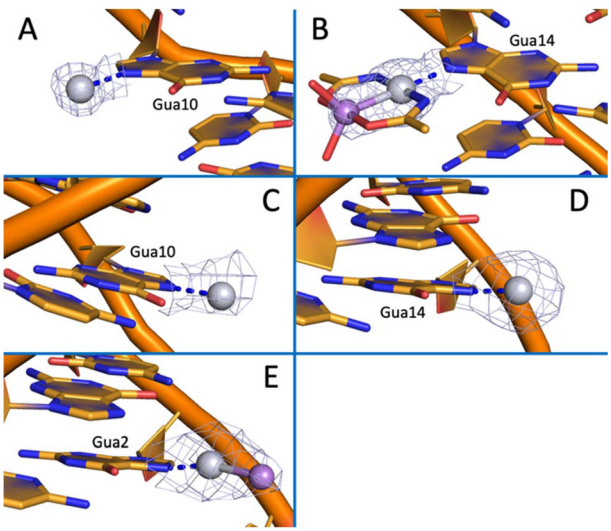

Fig. 5 Metal binding sites in the AP-1/DNA adducts obtained after 4 h and 48 h of soaking. In the AP-1/DNA adduct obtained after 4 h of soaking Pt was found close to (A) Gua10, while Pt and As were found close to (B) Gua14. In the AP-1/DNA adduct obtained after 48 h of soaking Pt was found close to (C) Gua10 and (D) Gua14, while Pt and As were found close to (E) Gua2. $2F_o - F_c$ electron density maps were recorded at 1.0σ. Anomalous difference electron density maps are presented in Fig. S3.†

bond was retained but metal ligands cannot be modelled. It is interesting to note that the Pt–As containing the fragment bound to Gua2 in the AP-1/DNA 48 h structure occupies almost the same position as adopted by a hexaaqua magnesium ion, which mediates the interaction with a symmetry-related molecule in the AP-1/DNA 4 h structure (Fig. S4†). The occupancy factors for the Pt atoms bound to Gua2, Gua10, and Gua14 in this structure are 0.25, 0.15, and 0.40, respectively. The *B*-factors and the Pt–N7 bond distances are within the ranges 62–87 $Å^2$ and 2.1–2.2 Å, respectively. The Pt–As bond length is 2.3 Å.

Electrospray ionization mass spectrometry data

The deconvoluted ESI MS spectrum of the untreated DNA duplex (in 100 mM ammonium acetate buffer; pH 6.8) is shown in Fig. 6A. Notably, the ESI MS experiment, in line with previous observations,[44] causes extensive separation of the two DNA strands so that the mass spectrum shows intense peaks for both the single strand (SS, 3645.713 Da) and the double strand (DS, 7290.466 Da) species. The ratio between the intensities of the two peaks may be finely tuned by adjusting the parameters of the ESI MS experiment. Ammonium ions can also bind SS and DS, so that additional peaks are detectable by ES-MS (3696.816 Da indicates SS + 3 NH_4^+, 7325.504 Da indicates DS + 2 NH_4^+, 7343.500 Da indicates DS + 3 NH_4^+). The experiment was then repeated following treatment of the double stranded DNA with cisplatin, transplatin or AP-1 under a variety of solution conditions.

We observed that cisplatin and transplatin manifest a strong tendency to form adducts with this DNA oligonucleotide (Fig. 6B and C). Cisplatin and transplatin were added at a 3 : 1 Pt : DS molar ratio and the adducts (mostly of 1 : 1 and 2 : 1 stoichiometry, respectively) were clearly seen after 3 h of incubation. Notably, the adducts were almost exclusively observed at the level of single stranded DNA, implying that the Pt/double strand dodecamer molar ratio in the adduct may be higher (we like to remind here that strand separation is just a consequence of the electrospray ionization process). The adducts formed between cisplatin/transplatin and this DNA structure are stable for 48 h (Fig. S5 and S6†); these results highlight the strength of the interaction occurring between platinum and DNA.

In the case of AP-1 a profoundly different situation emerges from the ESI MS experiments. In fact, at a 3 : 1 AP-1 : DS molar ratio, AP-1 was not able at all to produce adducts with this dodecameric DNA (Fig. S7†). An AP-1/DNA adduct could be obtained only at very large AP-1 to DS molar ratios (30 : 1, Fig. 6D). This adduct is consistent with the binding of two $[Pt(NHC(CH_3)O)_2As(OH)_2]^+$ units (AP-1 – Cl in Fig. 6D) to SS DNA. The stability of the adduct was tested for 48 h and again, no evidence of the breaking of the Pt–As bond was obtained in the ESI MS spectra during this time.

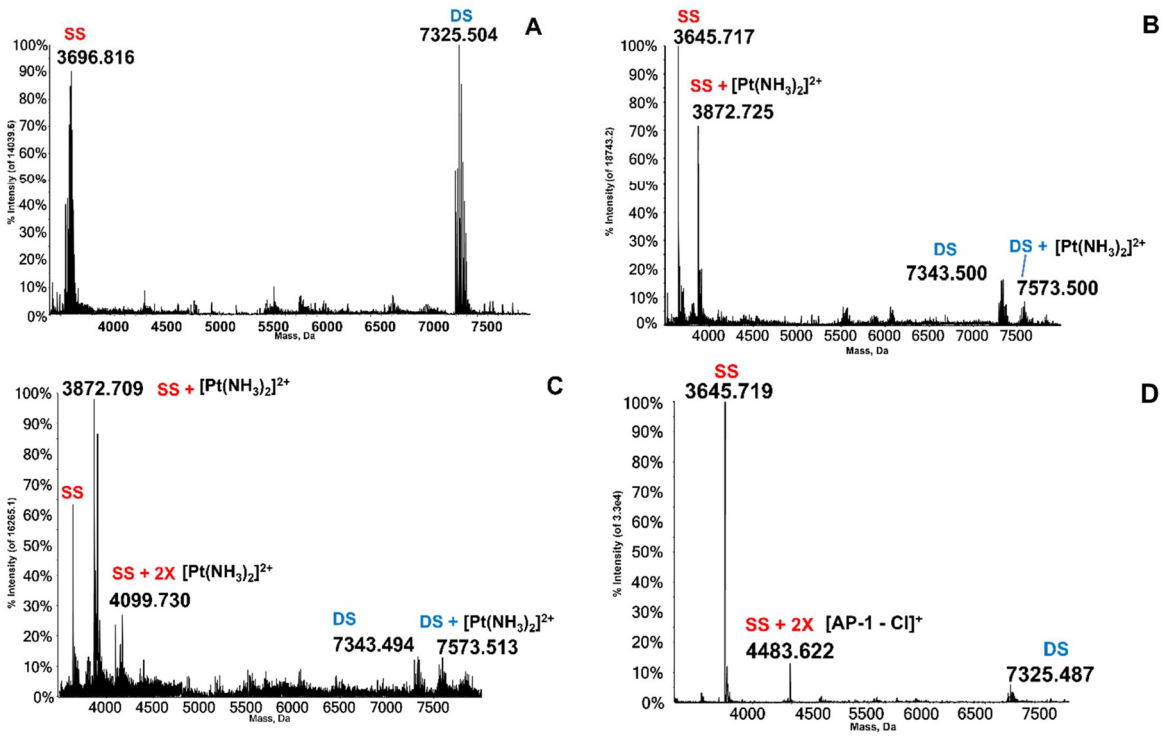

Fig. 6 ESI MS spectra of (A) the Dickerson sequence (5′-CGCGAATTCGCG-3′), (B) the Dickerson sequence and cisplatin; metal complex to DNA ratio 3 : 1, (C) the Dickerson sequence and transplatin, metal complex to DNA ratio 3 : 1, (D) the Dickerson sequence and AP-1, metal complex to DNA ratio 30 : 1, incubated for 3 h in 100 mM ammonium acetate buffer (pH = 6.8), at a concentration of 10^{-4} M.

Summary and conclusions

In conclusion, we have compared here the binding of cisplatin, transplatin and AP-1 to a popular double strand B-DNA dodecamer, the so-called Dickerson dodecamer. Crystallographic studies show that the three compounds interact with DNA through the binding of Pt to the N7 atom of a guanine base, upon the breaking of the Pt–Cl bond. However, they produce different final adducts in soaked crystals, in terms of the number and location of the Pt binding sites.

Our cisplatin/DNA structure presents one Pt binding site more than the structure of the same adduct previously reported.[41] This could be due to the differences in the sample preparation.

Depending on the soaking time, different numbers of Pt binding sites were observed in the transplatin/DNA and AP-1/DNA adducts. One or two Pt binding sites were observed in the adducts with transplatin, while two or three metal binding sites were found in the AP-1/DNA adducts. Furthermore, the occupancies of the Pt center in the adducts with transplatin are lower than those in the adduct with cisplatin. Three previously unobserved metal binding sites (Gua22 in the cisplatin/DNA adduct and Gua14 and Gua2 in the AP-1/DNA adducts) were found in the 5′-CGCGAATTCGCG-3′ sequence. Notably, in the AP-1/DNA adduct formed after 4 h of soaking, the Pt–As bond is retained in only one of two metal binding sites (close to Gua14), while in the other metal binding site there is no evidence of the presence of As. In contrast, in the structure of the AP-1/DNA adduct formed after soaking for 48 h, the Pt–As bond is identified only in the third additional metal binding site close to Gua2. Thus, the structural data suggest that the Pt–As bond can break down upon the interaction with the double helix. These structural results are in agreement with previous inductively plasma coupled mass data.[39] Indeed, it has already been demonstrated that when AP-1 is bound to the nuclear DNA of MDA-MB-231 cancer cells, the Pt : As ratio is close to 1 (0.97) after 4 h, while there are fewer moles of arsenic than platinum after 8 h of incubation.[39] This suggests that the Pt–As bond in AP-1/DNA adducts is intact at the early stage but dissociates at later times. The release of the $As(OH)_2$ fragment that occurs after the DNA binding could play an important role in the mechanism of action of arsenoplatins.

To achieve independent information on the investigated systems, ESI MS measurements were subsequently carried out. As previously reported,[44] the Dickerson dodecamer manifests a peculiar behavior in the ESI MS measurements; indeed, the ionization process produces partial separation of the two DNA strands that are directly monitored in the ESI MS spectra. Typically, DNA-bound metallodrugs are preferentially seen on the single strand species, probably in relation to their destabilizing effect. ESI MS experiments revealed that cisplatin and transplatin bind the Dickerson dodecamer. The results are not in complete agreement with those found from X-ray crystallography. The differences can be due to different conditions of the two experiments and to the peculiar behavior of the Dickerson dodecamer in the ESI MS measurements.

The binding experiments with AP-1 pointed out that this bifunctional compound is far less reactive than cisplatin with DNA under the applied solution conditions and that adducts with the Dickerson dodecamer may only be observed upon applying very large AP-1 to DS molar ratios (30 : 1 or more). The resulting adduct, showing a predominant 2 : 1 AP-1/SS stoichiometry, is stable for 48 h. At variance with the crystallographic data, no evidence is obtained in the ESI MS spectra of the possible cleavage of the Pt–As bond. Thus, we may hypothesize that the specific solution conditions of the ESI MS experiments disfavor the slow progressive cleavage of the Pt–As bond, observed with other techniques. Indeed, the entire adduct was retained and the displacement of the metal fragments, *i.e.* $[Pt(NHC(CH_3)O)_2As(OH)_2]^+$, or the cleavage of the Pt–As bond, did not occur during the time. In any case, these results support the idea that arsenoplatins have unique structures and mechanisms of action that provide them the ability to overcome cisplatin resistance[48] and the obstacles associated with the use of As_2O_3.[49–51]

Experimental

Materials

The 5′-CGCGAATTCGCG-3′ DNA sequence, for crystallization (HPLC grade) and ESI MS (desalted) experiments, was purchased from Eurogentec and Eurofins Genomics. Cisplatin, transplatin and all chemicals were purchased from Sigma-Aldrich (Merck). Arsenoplatin-1 (AP-1) was synthesized in MetMed laboratories at the Department of Chemistry, University of Florence following the protocol by Miodragović and coworkers.[37]

Crystallization

In order to form the duplex and ensure the homogeneity of samples, 1.9 mM (single strand concentration) DNA solutions were annealed in 20 mM sodium cacodylate at pH 7.0 by heating to 90 °C for 5 min and then slowly cooling down for 50–60 min and storing at 20 °C overnight. Crystals of d(5′-CGCGAATTCGCG-3′)$_2$ were grown using the hanging drop vapor diffusion method by mixing 0.5 μL of 0.95 mM DNA duplex and 0.5 μL of 7–14% (v/v) 2-methyl-2,4-pentanediol (MPD), 20 mM $MgCl_2$, 80 mM spermine tetrahydrochloride, and 60 mM sodium cacodylate pH 6.5. The crystallization solution was equilibrated at 20 °C against a reservoir containing 50–60% (v/v) MPD. Crystals of native B-DNA were soaked in crystallization solutions saturated with cisplatin (6 days), transplatin (4 h and 7 days) or AP-1 (48 h). AP-1/DNA adduct crystals were also obtained upon soaking for 4 h by exposing DNA crystals to a 50% (v/v) MPD solution containing 3.8 mM metal compound.

Data collection, structure determination, refinement, and structural analysis

Diffraction data for the cisplatin/DNA adduct were collected at the ID23-2 beamline of the European Synchrotron Radiation Facility (ESRF, Grenoble, France) at λ = 0.8731 Å. Diffraction

data for the other adducts were collected at the XRD2 beamline of Elettra Synchrotron in Trieste (Italy), at λ = 1.0000 Å. Datasets were processed using the autoPROC software.[52–56] The phase problem was solved by molecular replacement using the Phaser MR[57] or the MOLREP[58] program. The coordinates of native B-DNA (PDB code: 3U2N)[42] were used as a search model. Restrained refinements were carried out with REFMAC5[59] using the CCP4 package.[54] The Coot program[60] was used for the visualization of the electron density maps and for model building. The Pt binding site was identified using difference Fourier ($2F_o - F_c$ and $F_o - F_c$) and anomalous difference electron density maps. Pt and As occupancies were evaluated trying to minimize the positive and negative peaks on metal centers in the Fourier difference $F_o - F_c$ electron density maps and to obtain the best R_{factor} and R_{free} values. The structures were validated using the PDB validation server (**https://validate-rcsb-1.wwpdb.org/**) and Coot routines.[60] Root-mean-square deviations (RMSD) were calculated using the Superpose program (CCP4 package).[54] The coordinates of the cisplatin/DNA (PDB code 8C62), transplatin/DNA (PDB codes 8RI5 after 48 h of soaking and 8RI3 after 7 days of soaking) and AP-1/DNA adducts (PDB codes 8C63 upon 4 h of soaking and 8C64 after 48 h of soaking) were deposited in the Protein Data Bank (PDB). Detailed statistics on the data collection and refinement are reported in Table S1.† Molecular graphics figures were prepared with PyMOL (DeLano Scientific, Palo Alto, CA, USA).

Electrospray ionization mass spectrometry experiments

For the mass spectrometry measurements, all samples were prepared in LC-MS grade solvents or solutions. In order to form the duplex and to prepare a homogeneous sample, annealing of DNA was carried out as follows: 1 mM DNA (single strand concentration) in 100 mM ammonium acetate at pH 6.8 was kept at 90 °C for 5 min and then slowly cooled down for 50–60 min and stored at 20 °C overnight. For the reaction with the selected metal complex, an aliquot of the B-DNA duplex solution was mixed with an aliquot of 10^{-3} M cisplatin, transplatin or AP-1 solution and diluted with 100 mM ammonium acetate to a final concentration of 10^{-4} M and a DS DNA-to-metal molar ratio of 1 : 3 and 1 : 30, respectively. The obtained mixture was incubated at 37 °C. All samples were diluted to a final DS concentration of 5×10^{-6} M using 100 mM ammonium acetate solution. 20% methanol was added just before injection to acquire a stable electrospray signal.

ESI-MS investigations were performed using a TripleTOF® 5600+ high-resolution mass spectrometer (Sciex, Framingham, MA, U.S.A.), equipped with a DuoSpray® interface operating with an ESI probe. All the ESI mass spectra were acquired through direct infusion at a 7 μL min^{-1} flow rate. The ESI source parameters optimized for B-DNA are as follows: negative polarity, ion-spray voltage floating (ISFV) −4000 V, temperature (TEM) 0 °C, ion source gas 1 (GS1) 40 L min^{-1}; ion source gas 2 (GS2) 0 L min^{-1}; curtain gas (CUR) 30 L min^{-1}, collision energy (CE) −10 V; declustering potential (DP) −10 V, acquisition range 1000–2400 *m*/*z*.

For acquisition, the Analyst TF software 1.7.1 (Sciex) was used and deconvoluted spectra were obtained using the Bio tool kit micro-application v.2.2 embedded in the PeakView™ software v.2.2 (Sciex).

Author contributions

All authors have given approval to the final version of the manuscript. R. T. and G. T. have equally contributed to this work.

Conflicts of interest

There are no conflicts to declare.

Acknowledgements

The authors would like to thank the Elettra Sincrotrone Trieste and the European Synchrotron Radiation Facility (ESRF) for beamtime (proposals 20215895 and MX-2363), and the staff of XRD2 (Elettra) and ID23-2 (ESRF) beamlines for technical assistance during data collection. Lu. M. and La. M. gratefully acknowledge Beneficentia Stiftung, ITT (Istituto Toscano Tumori), Ente Cassa Risparmio Firenze (ECR), and AIRC (IG-16049) COST Action CM1105 for financial support, CISM (University of Florence) for ESI MS spectra. Lu. M., La. M., and A. G. gratefully acknowledge the Fondazione Italiana per la Ricerca sul Cancro (AIRC), Milan, and Fondazione Cassa Risparmio Firenze for funding the project "Advanced mass spectrometry tools for cancer research: novel applications in proteomics, metabolomics, and nanomedicine" (Multi-user Equipment Program 2016, ref. code 19650). Lu. M., La. M., and A. G. also thank AIRC, IG 2021 ID 26169 "Multi-Omics approach to establish the molecular mechanisms of Anticancer Gold Compounds in the Systems Biology Era".

References

1 B. Rosenberg, L. Van Camp and T. Krigas, *Nature*, 1965, **205**, 698–699.
2 S. J. Berners-Price, *Angew. Chem., Int. Ed.*, 2011, **50**, 804–805.
3 Y. Min, C. Mao, S. Chen, G. Ma, J. Wang and Y. Liu, *Angew. Chem.*, 2012, **124**, 6846–6851.
4 N. P. Farrell, *Chem. Soc. Rev.*, 2015, **44**, 8773–8785.
5 V. Calandrini, G. Rossetti, F. Arnesano, G. Natile and P. Carloni, *J. Inorg. Biochem.*, 2015, **153**, 231–238.
6 L. Gatti, G. Cassinelli, N. Zaffaroni, C. Lanzi and P. Perego, *Drug Resistance Updates*, 2015, **20**, 1–11.
7 D. Holmes, *Nature*, 2015, **527**, S218–S219.
8 S. Kachalaki, M. Ebrahimi, L. Mohamed Khosroshahi, S. Mohammadinejad and B. Baradaran, *Eur. J. Pharm. Sci.*, 2016, **89**, 20–30.

9 S. Chen, D. Xu, H. Jiang, Z. Xi, P. Zhu and Y. Liu, *Angew. Chem., Int. Ed.*, 2012, **51**, 12258–12262.
10 A. A. Legin, M. A. Jakupec, N. A. Bokach, M. R. Tyan, V. Yu. Kukushkin and B. K. Keppler, *J. Inorg. Biochem.*, 2014, **133**, 33–39.
11 H. Song, W. Li, R. Qi, L. Yan, X. Jing, M. Zheng and H. Xiao, *Chem. Commun.*, 2015, **51**, 11493–11495.
12 F. M. Muggia, A. Bonetti, J. D. Hoeschele, M. Rozencweig and S. B. Howell, *J. Clin. Oncol.*, 2015, **33**, 4219–4226.
13 M. Patra, T. C. Johnstone, K. Suntharalingam and S. J. Lippard, *Angew. Chem.*, 2016, **128**, 2596–2600.
14 I. Ott and R. Gust, *Arch. Pharm.*, 2007, **340**, 117–126.
15 S. Spreckelmeyer, C. Orvig and A. Casini, *Molecules*, 2014, **19**, 15584–15610.
16 E. J. Anthony, E. M. Bolitho, H. E. Bridgewater, O. W. L. Carter, J. M. Donnelly, C. Imberti, E. C. Lant, F. Lermyte, R. J. Needham, M. Palau, P. J. Sadler, H. Shi, F.-X. Wang, W.-Y. Zhang and Z. Zhang, *Chem. Sci.*, 2020, **11**, 12888–12917.
17 M. G. Ferraro, M. Piccolo, G. Misso, R. Santamaria and C. Irace, *Pharmaceutics*, 2022, **14**, 954.
18 D. M. Monti, G. Ferraro and A. Merlino, *Nanomedicine*, 2019, **20**, 101997.
19 D. M. Monti, D. Loreto, I. Iacobucci, G. Ferraro, A. Pratesi, L. D'Elia, M. Monti and A. Merlino, *Pharmaceuticals*, 2022, **15**, 425.
20 L. S. Mangala, V. Zuzel, R. Schmandt, E. S. Leshane, J. B. Halder, G. N. Armaiz-Pena, W. A. Spannuth, T. Tanaka, M. M. K. Shahzad, Y. G. Lin, A. M. Nick, C. G. Danes, J.-W. Lee, N. B. Jennings, P. E. Vivas-Mejia, J. K. Wolf, R. L. Coleman, Z. H. Siddik, G. Lopez-Berestein, S. Lutsenko and A. K. Sood, *Clin. Cancer Res.*, 2009, **15**, 3770–3780.
21 M. Poursharifi, M. T. Wlodarczyk and A. J. Mieszawska, *Inorganics*, 2018, **7**, 2.
22 A. Pöthig and A. Casini, *Theranostics*, 2019, **9**, 3150–3169.
23 H. Li, X. Zhu, Y. Zhang, J. Xiang and H. Chen, *J. Exp. Clin. Cancer Res.*, 2009, **28**, 110.
24 J. C. Barnes, P. M. Bruno, H. V.-T. Nguyen, L. Liao, J. Liu, M. T. Hemann and J. A. Johnson, *J. Am. Chem. Soc.*, 2016, **138**, 12494–12501.
25 W. A. Wani, S. Prashar, S. Shreaz and S. Gómez-Ruiz, *Coord. Chem. Rev.*, 2016, **312**, 67–98.
26 Y. Gou, G. Huang, J. Li, F. Yang and H. Liang, *Coord. Chem. Rev.*, 2021, **441**, 213975.
27 E. P. Swindell, P. L. Hankins, H. Chen, Đ. U. Miodragović and T. V. O'Halloran, *Inorg. Chem.*, 2013, **52**, 12292–12304.
28 S. M. Cohen and S. J. Lippard, in *Prog. Nucleic Acid Res. Mol. Biol*, Elsevier, 2001, vol. 67, pp. 93–130.
29 J. Zhu, Z. Chen, V. Lallemand-Breitenbach and H. de Thé, *Nat. Rev. Cancer*, 2002, **2**, 705–713.
30 X.-W. Zhang, X.-J. Yan, Z.-R. Zhou, F.-F. Yang, Z.-Y. Wu, H.-B. Sun, W.-X. Liang, A.-X. Song, V. Lallemand-Breitenbach, M. Jeanne, Q.-Y. Zhang, H.-Y. Yang, Q.-H. Huang, G.-B. Zhou, J.-H. Tong, Y. Zhang, J.-H. Wu, H.-Y. Hu, H. de Thé, S.-J. Chen and Z. Chen, *Science*, 2010, **328**, 240–243.
31 J. Zhu, Z. Chen, V. Lallemand-Breitenbach and H. De Thé, *Nat. Rev. Cancer*, 2002, **2**, 705–714.
32 A. A. E. Ali, G. Timinszky, R. Arribas-Bosacoma, M. Kozlowski, P. O. Hassa, M. Hassler, A. G. Ladurner, L. H. Pearl and A. W. Oliver, *Nat. Struct. Mol. Biol.*, 2012, **19**, 685–692.
33 X. Zhou, X. Sun, C. Mobarak, A. J. Gandolfi, S. W. Burchiel, L. G. Hudson and K. J. Liu, *Chem. Res. Toxicol.*, 2014, **27**, 690–698.
34 C. Muenyi, M. Ljungman and J. States, *Biomolecules*, 2015, **5**, 2184–2193.
35 N. Zhang, Z. Wu, E. McGowan, J. Shi, Z. Hong, C. Ding, P. Xia and W. Di, *Cancer Sci.*, 2009, **100**, 2459–2464.
36 T. Nakaoka, A. Ota, T. Ono, S. Karnan, H. Konishi, A. Furuhashi, Y. Ohmura, Y. Yamada, Y. Hosokawa and Y. Kazaoka, *Cell. Oncol.*, 2014, **37**, 119–129.
37 Đ. Miodragović, J. A. Quentzel, J. W. Kurutz, C. L. Stern, R. W. Ahn, I. Kandela, A. Mazar and T. V. O'Halloran, *Angew. Chem., Int. Ed.*, 2013, **52**, 10749–10752.
38 Đ. Miodragović, E. P. Swindell, Z. Sattar Waxali, A. Bogachkov and T. V. O'Halloran, *Inorg. Chim. Acta*, 2019, **496**, 119030.
39 Đ. Miodragović, A. Merlino, E. P. Swindell, A. Bogachkov, R. W. Ahn, S. Abuhadba, G. Ferraro, T. Marzo, A. P. Mazar, L. Messori and T. V. O'Halloran, *J. Am. Chem. Soc.*, 2019, **141**, 6453–6457.
40 I. Tolbatov, D. Cirri, M. Tarchi, T. Marzo, C. Coletti, A. Marrone, L. Messori, N. Re and L. Massai, *Inorg. Chem.*, 2022, **61**, 3240–3248.
41 R. M. Wing, P. Pjura, H. R. Drew and R. E. Dickerson, *EMBO J.*, 1984, **3**, 1201–1206.
42 D. Wei, W. D. Wilson and S. Neidle, *J. Am. Chem. Soc.*, 2013, **135**, 1369–1377.
43 M. Coluccia and G. Natile, *Anti-Cancer Agents Med. Chem.*, 2007, **7**, 111–123.
44 G. Tito, R. Troisi, G. Ferraro, A. Geri, L. Massai, L. Messori, F. Sica and A. Merlino, *Dalton Trans.*, 2023, **52**, 6992–6996.
45 T. Kishimoto, Y. Yoshikawa, K. Yoshikawa and S. Komeda, *Int. J. Mol. Sci.*, 2019, **21**, 34.
46 E. Bernal-Méndez, M. Boudvillain, F. González-Vílchez and M. Leng, *Biochemistry*, 1997, **36**, 7281–7287.
47 M. Boudvillain, R. Dalbiès, C. Aussourd and M. Leng, *Nucleic Acids Res.*, 1995, **23**, 2381–2388.
48 D.-W. Shen, L. M. Pouliot, M. D. Hall and M. M. Gottesman, *Pharmacol. Rev.*, 2012, **64**, 706–721.
49 E. P. Swindell, P. L. Hankins, H. Chen, D. U. Miodragović and T. V. O'Halloran, *Inorg. Chem.*, 2013, **52**, 12292–12304.
50 Z. Zhang, H. Liu, H. Zhou, X. Zhu, Z. Zhao, X. Chi, H. Shan and J. Gao, *Nanoscale*, 2016, **8**, 4373–4380.
51 X. Wu, Z. Han, R. M. Schur and Z.-R. Lu, *ACS Biomater. Sci. Eng.*, 2016, **2**, 501–507.
52 P. Evans, *Acta Crystallogr., Sect. D: Biol. Crystallogr.*, 2006, **62**, 72–82.
53 W. Kabsch, *Acta Crystallogr., Sect. D: Biol. Crystallogr.*, 2010, **66**, 125–132.

54 M. D. Winn, C. C. Ballard, K. D. Cowtan, E. J. Dodson, P. Emsley, P. R. Evans, R. M. Keegan, E. B. Krissinel, A. G. W. Leslie, A. McCoy, S. J. McNicholas, G. N. Murshudov, N. S. Pannu, E. A. Potterton, H. R. Powell, R. J. Read, A. Vagin and K. S. Wilson, *Acta Crystallogr., Sect. D: Biol. Crystallogr.*, 2011, **67**, 235–242.
55 C. Vonrhein, C. Flensburg, P. Keller, A. Sharff, O. Smart, W. Paciorek, T. Womack and G. Bricogne, *Acta Crystallogr., Sect. D: Biol. Crystallogr.*, 2011, **67**, 293–302.
56 P. R. Evans and G. N. Murshudov, *Acta Crystallogr., Sect. D: Biol. Crystallogr.*, 2013, **69**, 1204–1214.
57 A. J. McCoy, R. W. Grosse-Kunstleve, P. D. Adams, M. D. Winn, L. C. Storoni and R. J. Read, *J. Appl. Crystallogr.*, 2007, **40**, 658–674.
58 A. Vagin and A. Teplyakov, *Acta Crystallogr., Sect. D: Biol. Crystallogr.*, 2010, **66**, 22–25.
59 G. N. Murshudov, P. Skubák, A. A. Lebedev, N. S. Pannu, R. A. Steiner, R. A. Nicholls, M. D. Winn, F. Long and A. A. Vagin, *Acta Crystallogr., Sect. D: Biol. Crystallogr.*, 2011, **67**, 355–367.
60 P. Emsley, B. Lohkamp, W. G. Scott and K. Cowtan, *Acta Crystallogr., Sect. D: Biol. Crystallogr.*, 2010, **66**, 486–501.